



**An Effective Penetration Shield Design for ICF Reactors**

**M.E. Sawan, W.F. Vogelsang, and D.K. Sze**

**May 1983**

**FPA-83-2**

**FUSION POWER ASSOCIATES**

**2 Professional Drive, Suite 248  
Gaithersburg, Maryland 20879  
(301) 258-0545**

**1500 Engineering Drive  
Madison, Wisconsin 53706  
(608) 263-2308**

AN EFFECTIVE PENETRATION SHIELD DESIGN  
FOR ICF REACTORS

M.E. Sawan, W.F. Vogelsang, and D.K. Sze  
Nuclear Engineering Department, The University of Wisconsin  
Madison, Wisconsin, U.S.A.

ABSTRACT

A shield design in which the inner surface is tapered along the direct line-of-sight from the ICF target is presented. This shield design was found to reduce the radiation effects in the final focussing magnets of HIBALL by three orders of magnitude compared to the traditional untapered shield design. This design results also in reducing radiation streaming into the periodic transport system of HIBALL.

---

INTRODUCTION

An inertial confinement fusion (ICF) reactor must have penetrations in the reactor cavity walls to allow the beams (ions, electrons, or laser light) to strike the target.<sup>1,2,3</sup> After ignition, the radiation from the target will stream out through these penetrations into the beam lines and measures must be taken to protect vital components from this radiation. In this work, recognizing that because of the small target size (~ 6 mm) the radiation is essentially from a point source, we present a beam line shield design which is especially effective for the protection of the final focussing magnets in a heavy ion beam driven reactor and which may have application to other ICF concepts.

The HIBALL reactor, considered in this work, utilizes twenty 10 GeV Bi<sup>++</sup> ion beams to bring the target to ignition. Each beam port is rectangular in shape with a height of 1.03 m and a width of 0.34 m at the reactor cavity wall of radius 7 m. The beam ports occupy 1.14% of the  $4\pi$  solid angle at the target. A number of superconducting magnets are arranged along the beam line to focus the ion beam to a spot 6 mm in diameter at the target. Adequate shielding is required to reduce the radiation effects in the magnets below the established design limits. Various beam line penetration shield shapes have been considered to assess their effectiveness in reducing the radiation effects in the HIBALL beam focussing magnets.

CALCULATIONAL MODEL

A vertical cross section of HIBALL is shown in Fig. 1. The blanket region is 2 m thick and consists of SiC tubes through which Li<sub>17</sub>Pb<sub>83</sub> liquid metal eutectic flows. The tubes occupy 33% of the blanket region. A cylindrical vacuum wall having a radius of 7 m is used. Immediately behind the vacuum wall is a 0.4 m thick reflector composed of 90 v/o ferritic steel structure and 10 v/o Li<sub>17</sub>Pb<sub>83</sub> coolant. The reactor utilizes a 2.9 m thick concrete bio

logical shield. The results presented here are based on a DT yield of 400 MJ and a repetition rate of 5 Hz yielding  $7.1 \times 10^{20}$  fusion neutrons per second. Neutron multiplication, spectrum softening and gamma production in the target have been taken into account by performing one-dimensional neutronics and photonics calculations in the spherical target using the discrete ordinates code ANISN.<sup>4</sup>

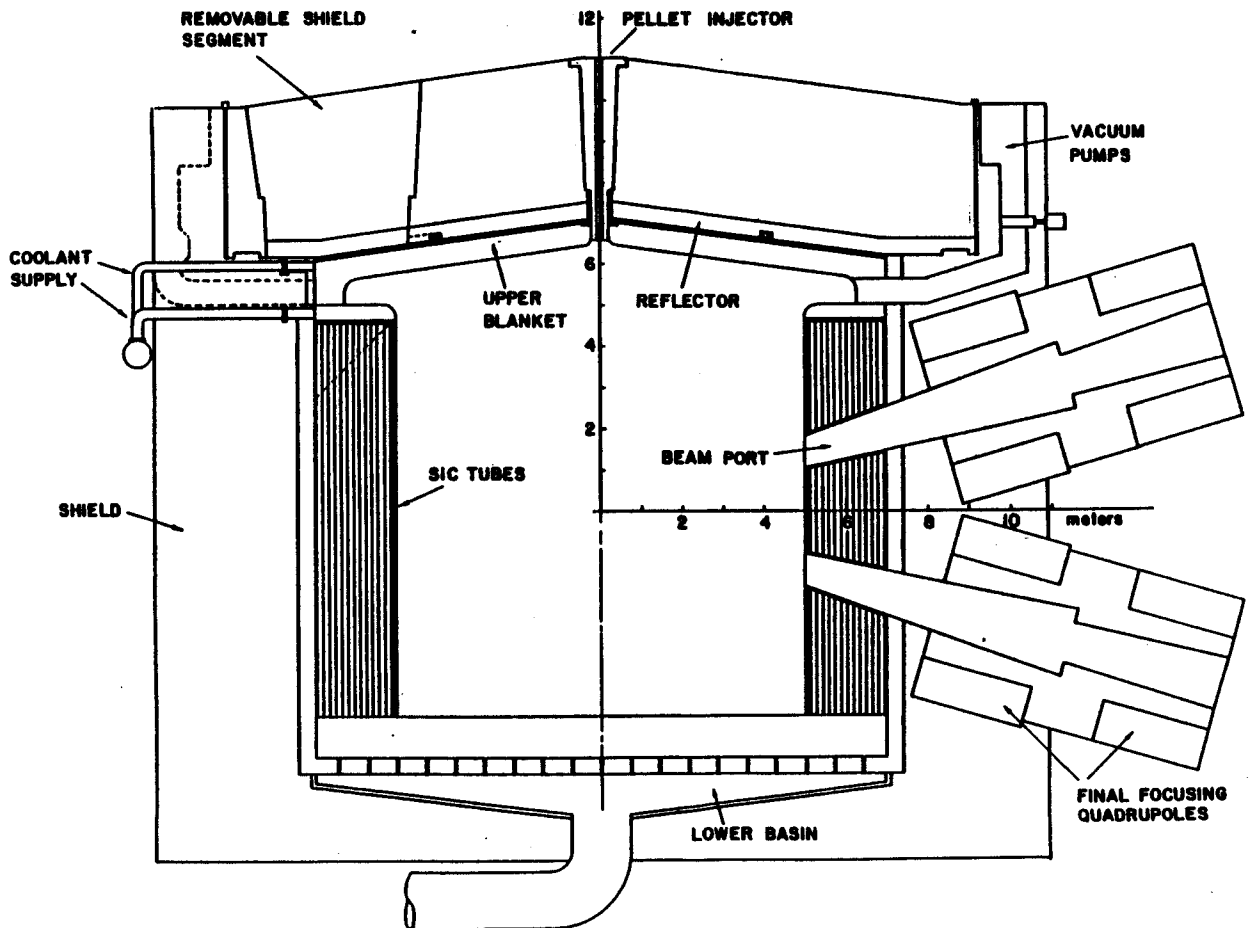


Fig. 1. A Vertical Cross Section of the HIBALL Reactor.

The initial design of the final beam transport system in HIBALL which focusses the beam from the periodic beam line onto the target, consists of eight quadrupole magnets. The total length of the system is 60.4 m. Each quadrupole has a length of 2.7 m with the drift sections between the quadrupoles being 1.8 m long. Figure 2 shows the vertical and horizontal envelopes for the beam as it is transported from the periodic line to the target. The positions of the eight quadrupoles used for focussing the beam are also shown. The inner dimensions of the magnet shield have been chosen to be at least 2 cm larger than the beam size, determined by the envelopes in Fig. 2, at all places along the penetration.

The 20 beam ports are arranged in two rows which are symmetric about the reactor midplane ( $z=0$ ). The beam ports are 4 m apart vertically at the reactor

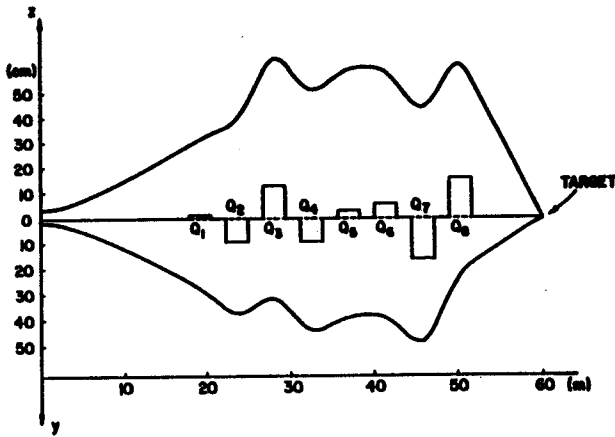


Fig. 2. Vertical and Horizontal  $\text{Bi}^{++}$  Ion Beam Envelopes.

coolant. The shield has a minimum thickness of 0.5 m in the quadrupole sections. The inner surface of the shield in the quadrupole section was tapered such that it does not see any direct line-of-sight source neutrons. This will be shown to be more advantageous than using a shield with a flat inner surface.

vacuum wall. Because of symmetry only half a penetration was modelled in the present analysis with reflecting albedo boundaries used at the planes of symmetry. Consequently, only 1/40 of the reactor was modelled. This corresponds to a "pie slice" of the upper half of the reactor with an azimuthal angle of  $18^\circ$ . The angle between the centerline of the beam line penetration and the reactor midplane is  $16^\circ$ . Each magnet coil was modelled as having 7.52 v/o NbTi superconductor, 67.48 v/o copper stabilizer, 15 v/o liquid helium coolant, and 10 v/o epoxy insulator. The magnet shield was taken to be 63 v/o type 316 stainless steel, 15 v/o lead, 17 v/o  $\text{B}_4\text{C}$  and 5 v/o  $\text{H}_2\text{O}$

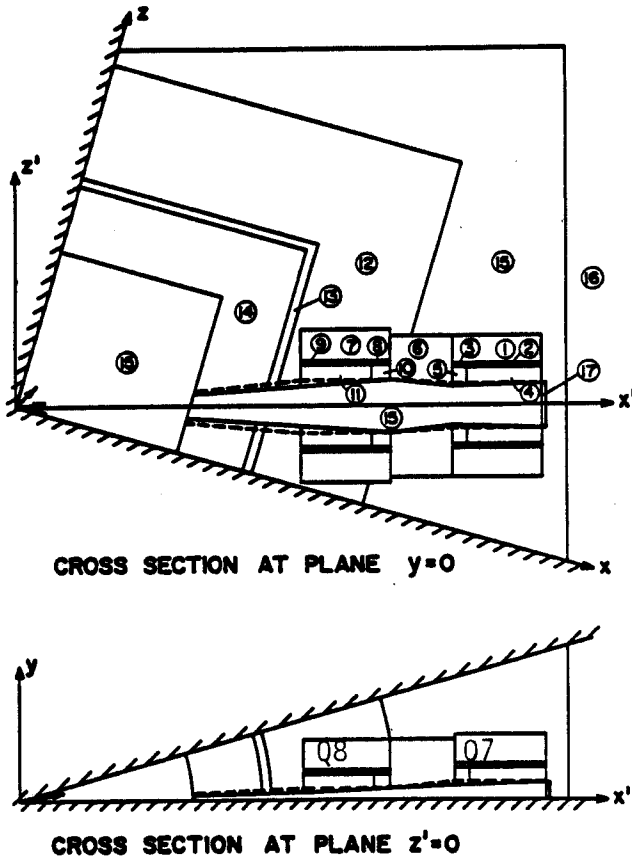


Fig. 3. Geometry of Computational Model for Final Two Focussing Magnets.

Zone 12 represents the biological shield. Zones 13 and 14 represent the reflector and

The neutronics and photonics calculations were performed using the three-dimensional Monte Carlo code MORSE.<sup>5</sup> A coupled 25 neutron - 21 gamma group cross section library was used. The library consists of the RSIC DLC-41B/VITAMIN-C data library<sup>6</sup> and the DLC-60/MACKLIB-IV response data library.<sup>7</sup> The results of the separate target calculations were used to define the isotropic point source at the origin of the Monte Carlo problem. In order to get statistically adequate estimates for the flux in the focussing magnets with a reasonable number of histories, an angular biasing technique was used.

Because of the  $1/R^2$  geometrical attenuation, the largest radiation effects occur in the magnets closer to the source. For this reason and to reduce the computing time, only the final two quadrupoles Q7 and Q8 were modelled. The geometry for the computational model used in this work is given in Fig. 3. Each quadrupole was divided into two zones. Zone 12

blanket, respectively. The inner vacuum region (zone 15) was extended to the region outside the biological shield and the focussing magnets. This allows the neutrons leaking out of the biological shield to have additional collisions in the focussing magnets instead of being discarded as they would be if an outer vacuum region was used. The dashed lines in Fig. 3 represent the geometry for a flat shield in the quadrupole sections. The solid lines represent the case with the shield being tapered in the quadrupole sections. The results presented here were obtained using 20,000 histories in each Monte Carlo problem.

#### EFFECT OF SHIELD INNER SURFACE GEOMETRY

The effect of tapering the shield in the quadrupole sections on the flux in the magnets was investigated. The geometrical models used for the flat and tapered shield cases are shown in Fig. 3. In the tapered shield case, the shield is tapered along the direct line-of-sight of source neutrons. In this case, no direct source neutrons impinge on the part of the shield in the quadrupole sections. All source neutrons impinge on the inner surface of the shield in the drift section. Table 1 shows the effect of tapering the shield on the neutron scalar flux in the different zones.

Table 1. Effect of Shield Tapering on Flux Estimates

Region	Zone Number	Neutron Scalar Flux ( $n/m^2 s$ )	
		Flat Shield	Tapered Shield
<u>Q<sub>7</sub></u>	1	2.767x10 <sup>12</sup> (0.60) <sup>a</sup>	1.631x10 <sup>12</sup> (0.77)
	2	4.504x10 <sup>13</sup> (0.40)	3.441x10 <sup>13</sup> (0.52)
	3	2.156x10 <sup>14</sup> (0.38)	1.217x10 <sup>14</sup> (0.48)
<u>Shield for Q<sub>7</sub></u>	4	1.552x10 <sup>16</sup> (0.13)	7.728x10 <sup>15</sup> (0.14)
	5	3.606x10 <sup>16</sup> (0.17)	2.224x10 <sup>16</sup> (0.15)
<u>Drift Section Shield</u>	6	1.299x10 <sup>16</sup> (0.09)	9.765x10 <sup>15</sup> (0.08)
<u>Q<sub>8</sub></u>	7	7.388x10 <sup>13</sup> (0.75)	9.720x10 <sup>10</sup> (0.77)
	8	9.854x10 <sup>14</sup> (0.76)	9.758x10 <sup>13</sup> (0.69)
	9	1.780x10 <sup>15</sup> (0.50)	NS <sup>b</sup>
<u>Shield for Q<sub>8</sub></u>	10	6.624x10 <sup>16</sup> (0.14)	8.108x10 <sup>15</sup> (0.18)
	11	8.181x10 <sup>16</sup> (0.11)	1.980x10 <sup>15</sup> (0.30)

<sup>a</sup>Numbers in parentheses are fractional standard deviations.

<sup>b</sup>No score in this zone for the 20,000 histories used.

It is clear from the results in Table 1 that tapering the shield in the

quadrupole sections results in reducing the neutron flux in the magnets. The peak neutron flux in  $Q_7$  occurring in zone 3 is reduced by a factor of 1.8. On the other hand, the peak neutron flux in  $Q_8$  occurring in zone 8 is reduced by an order of magnitude. The effect of shield tapering on the flux in  $Q_8$  is more pronounced than that in  $Q_7$  because scattering of high energy neutrons is highly forward peaked. It is clear also that the flux in the shield for  $Q_8$  is reduced significantly by tapering. The reason is that in the tapered case no direct line-of-sight source neutrons reach zones 10 and 11 and neutrons reach these zones only after having collisions in the drift section shield (zone 6). On the other hand, the neutron flux in the shield for  $Q_7$  decreases only slightly because the source neutrons have a larger chance to go in the forward direction into zones 4 and 5 than to go in the backward direction into zones 10 and 11 after colliding in the drift section (zone 6). The neutron flux at the first surface of the HIBALL blanket at the reactor midplane is  $2.364 \times 10^{18} \text{ n/m}^2 \text{ s}$ . This implies that the peak flux in the focussing magnets is more than four orders of magnitude lower than the flux at the first surface of the blanket.

Further modification in the shape of the shield in the drift section may be made to improve the effectiveness of the magnet shield. The inner surface of the shield in the drift section is tapered at both ends such that it coincides with the direct line-of-sight from the source as shown in Fig. 4. In this case, all source neutrons impinge on a vertical neutron dump in the shield. This results in increasing the minimum distance between the magnet and the point on the surface of the shield where the source neutron has its first collision and is expected to reduce the radiation damage in the magnets. Two positions were considered for the neutron dump as shown in Fig. 4.

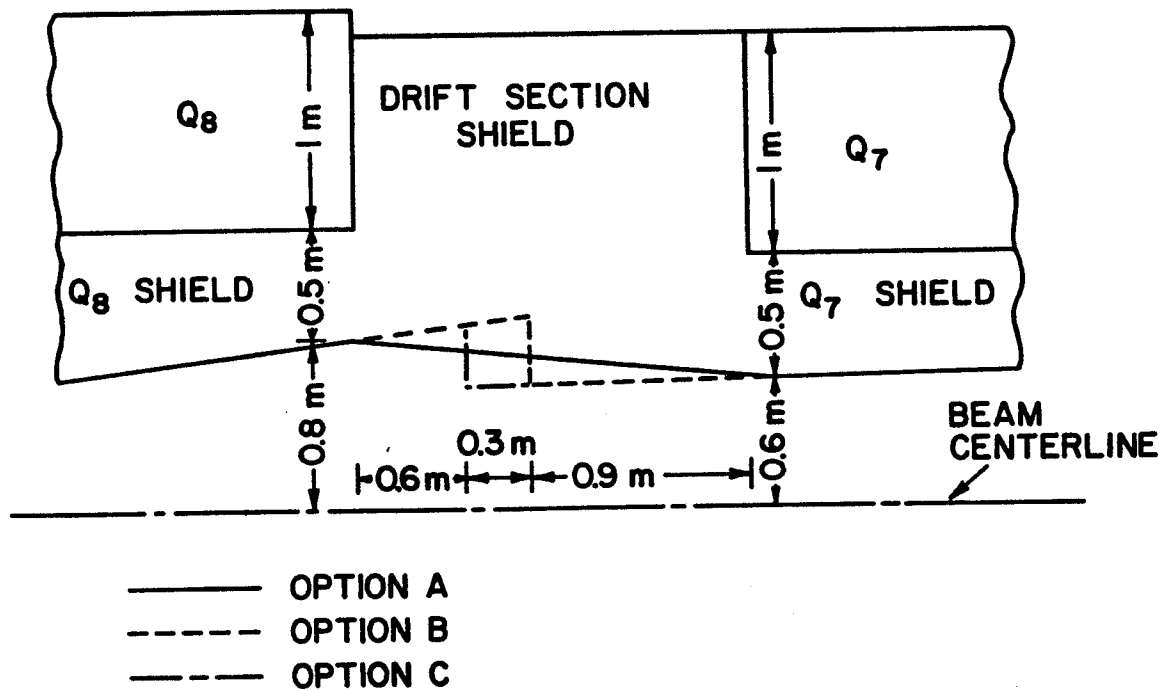


Fig. 4. Options for Tapering the Inner Surface of Shield in the Drift Section.

Table 2 gives the peak dpa rate, the peak radiation dose, and the peak power density in the focussing magnets for the different geometrical options considered. It is clear that the tapered shield with option C is the most effective shield design. Using option C for the drift section shield results in a peak Cu stabilizer dpa rate of only  $4.483 \times 10^{-6}$  displacements per atom (dpa)/full power year (FPY).

Table 2. Effect of Shield Inner Surface Geometry on Radiation Effects in Magnets

	Flat Shield	Tapered Shield in Quadrupole Section		
		Option A	Option B	Option C
Peak dpa/FPY in Cu Stabilizer	$1.056 \times 10^{-3}$	$1.151 \times 10^{-4}$	$1.600 \times 10^{-5}$	$4.480 \times 10^{-6}$
Peak Radiation Dose in Insulator	$3.467 \times 10^9$	$2.552 \times 10^8$	$2.526 \times 10^7$	$7.200 \times 10^6$
Peak Power Density ( $W/cm^3$ )	$4.380 \times 10^{-3}$	$2.44 \times 10^{-4}$	$3.554 \times 10^{-6}$	$5.350 \times 10^{-7}$

The limits on the radiation effects in superconducting magnets are design dependent. The magnetic field at the coils is less than one tesla. For OFHC copper with residual resistivity ratio of 107, the atomic displacements should not exceed  $2 \times 10^{-4}$  dpa for the resistivity not to exceed  $5 \times 10^{-10} \Omega m$  in a 1-tesla field. However, partial recovery of the radiation induced defects can be obtained by room temperature annealing. Increasing the time span between required anneals is desirable for increasing reactor availability. Decreasing the number of anneals required during the reactor lifetime also minimizes any possible undesirable consequences of cyclic irradiation. Using the shield design with option C, the maximum period of operation without annealing is  $\sim 45$  FPY. This is compared to 12.5 FPY when option B is used and  $\sim 17$  FPY when option A is used. If an untapered shield design is used, one needs to anneal the magnets after  $\sim 2$  months. This implies that when the shield design with option C is used, no annealing is needed for the estimated reactor life of 21 FPY (30 years at 70% capacity factor).

The radiation effects on the insulator are not reversible and it is essential that it lasts the whole reactor life. The design limit used for the radiation dose in the epoxy electrical insulator is  $4 \times 10^8$  rad. The results show that for an estimated reactor lifetime of 21 FPY, only the design with option C results in an accumulated radiation dose below the design limit. The design limit on the magnet heat load is set to be  $10^{-4} W/cm^3$ . It is clear from the results of Table 2 that the tapered shield design with options B and C satisfy this design criterion.

It is concluded from the results presented here that a magnet shield which is tapered in the quadrupole sections with option C for the drift section

shield shape satisfies the design criteria on the radiation dose in the insulator and the nuclear heating in the magnet with the possibility of eliminating the need for magnet annealing during the whole reactor lifetime. The minor modifications in the shield shape proposed here result in peak radiation effects in the magnets which are about three orders of magnitude less than those obtained when the traditional untapered shield is used.

Neutron streaming was followed up the beam line penetration to the exit of the periodic transport 60.4 m from the target. Fig. 5 shows the geometrical model used in this calculation. A trapping surface was used at the exit of the periodic transport to determine the amount of radiation streaming.  $2 \times 10^{14}$  neutrons were found to stream per second with approximately 37% of them coming directly from the target. The corresponding streaming current is  $4.4 \times 10^{10}$  n/m<sup>2</sup> s with an average energy of 11.7 MeV. The shield design used here was found also to reduce neutron streaming into the periodic transport by about a factor of two compared to the traditional untapered shield design.

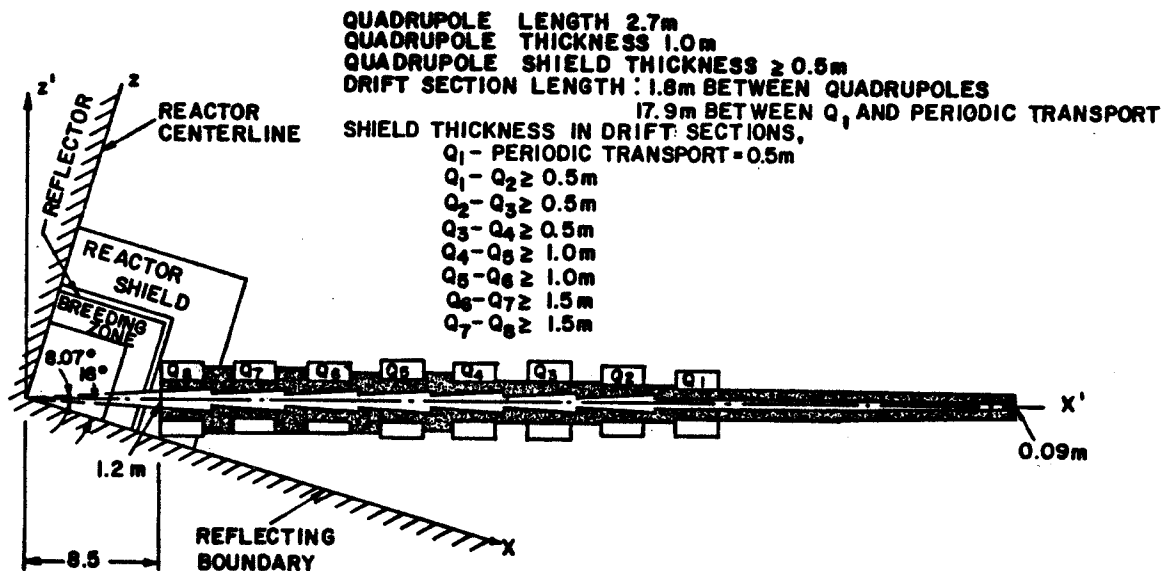


Fig. 5. Vertical Cross Section of the Beam Line Penetration in HIBALL.

#### APPLICATION TO THE IMPROVED FINAL FOUSSING SYSTEM OF HIBALL

Further study of the HIBALL accelerator, beam storage, and transport systems led to a new design using Bi<sup>+</sup> ions and resulted in a revised and improved (with respect to shielding) final focussing system. This system is 100 m long and consists of six quadrupole lenses and two deflection magnet sectors. The vertical and horizontal envelopes of the ion beam are shown in Fig. 6. The shield configuration along the penetration was determined using these envelopes and the tapered type of shield design proposed for the Bi<sup>++</sup> system. This leads



to a number of neutron dumps along the penetration. In this configuration, a minimum shield thickness of 0.3 m was maintained along the penetration.

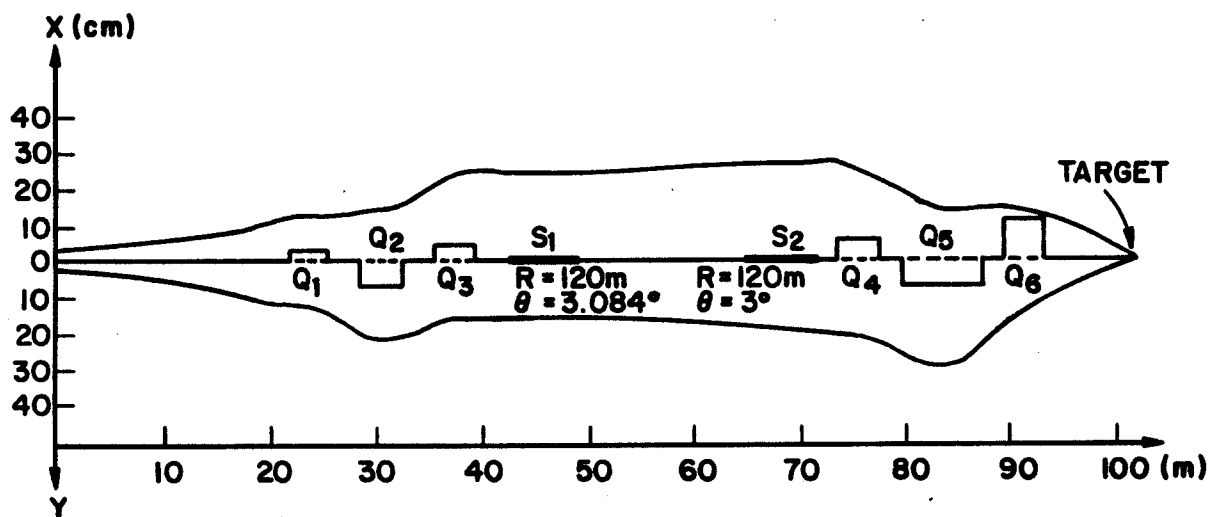


Fig. 6. Vertical and Horizontal  $\text{Bi}^+$  Ion Beam Envelopes.

This revised accelerator and final focussing system have several attractive features. The phase space volume for the ion beam is reduced resulting in reduced quadrupole apertures. Consequently, the beam port size at the vacuum wall is reduced by a factor of  $\sim 10$  leading to significant reduction in radiation streaming. Furthermore, the reduced aperture permits the use of smaller magnets. The angle between beams is reduced from  $32^\circ$  to  $16^\circ$ . This, together with the vertical beam offset provided by the two dipole magnets, results in reduced beam elevation. The beam offset also results in all direct streaming source neutrons ( $\bar{E} \sim 12 \text{ MeV}$ ) making their first collision in the final focussing system thus concealing the periodic transport from direct line-of-sight of source neutrons. The initial collisions for these neutrons take place in the four neutron dumps along the beam line penetration with most of the source neutrons interacting in a large final dump 46.5 m from the target between the two bending sectors.

To assess the shielding requirements for the superconducting and normal conductor coils, only the final two quadrupoles, where the largest radiation effects occur, were modelled. 40,000 histories were used in the calculation. In this modified system, the final magnet is driven by normal coils where the limits on the neutron fluence ( $E > 0.1 \text{ MeV}$ ) and instantaneous dose rate in the MgO insulator were considered to be  $1.1 \times 10^{26} \text{ n/m}^2$  and  $10^4 \text{ rad/s}$ , respectively. The radiation effects were calculated for both normal and superconducting coils to investigate the possibility of replacing one type by the other.

The peak radiation effects in the final two magnets are given in Table 3. It is clear that the radiation effects in the normal coils are much lower than the design limits suggesting that a reduced shield thickness can be used with normal coils resulting in further reduction in magnet size. The results also indicate that if superconducting coils are used in the final magnet, the more

radiation resistant polyimide insulator must replace epoxy. All other radiation effects are below the design limits.

Table 3. Radiation Effects in Final Two Magnets

	Final Magnet	Preceding Magnet
<u>Superconducting Coils</u>		
DPA in Cu Stabilizer (dpa/FPY)	$1.8 \times 10^{-5}$	$3.1 \times 10^{-6}$
Dose Rate in Insulator (rad/FPY)	$3 \times 10^7$	$6.3 \times 10^6$
Power Density in Magnet ( $W/cm^3$ )	$7.6 \times 10^{-6}$	$1.8 \times 10^{-6}$
<u>Normal Coils</u>		
Neutron Fluence ( $E > 0.1$ MeV) after 21 FPY ( $n/m^2$ )	$6.72 \times 10^{21}$	$1.05 \times 10^{21}$
Instantaneous Dose Rate in MgO (rad/s)	1.0	0.16

To quantify radiation streaming along the penetration, the computational model was modified to represent the penetration up to the final neutron dump. Particles crossing the trapping surface at the duct opening 46.5 m from the target were counted to determine the amount, and energy spectrum of streaming radiation. The neutron streaming current through the duct opening at the position of the final dump is  $6.68 \times 10^{15} n/m^2 s$  which is an order of magnitude less than the streaming current into the periodic transport of the previous design. Furthermore, the spectrum here is much softer with an average energy of 0.77 MeV. Further reduction in both streaming current and average energy will result as the neutrons travel farther up the beam line penetration to the periodic transport 100 m from the target. It was estimated that the neutron streaming current will be reduced by at least another three orders of magnitude and there will be additional spectrum softening.

#### SUMMARY AND CONCLUSIONS

A three-dimensional neutronics and photonics analysis was performed for the heavy ion beam line penetration in the HIBALL fusion reactor. Various penetration shield geometrical options were considered to assess their effectiveness in reducing the radiation effects in the beam focussing magnets. Tapering the shield in the quadrupole sections in such a way that all direct line-of-sight source neutrons fall on the inner surface of the drift section shield was found to reduce the radiation damage in the magnets. Several options for the shape of the shield in the drift sections were analyzed. The smallest radiation effects in the magnet were obtained when the inner surface of the shield in the drift section is also tapered resulting in a vertical neutron dump between the magnets. Better shielding was obtained with the neutron dump between the final two quadrupoles placed closer to the final

quadrupole. With this design, the period required before the first magnet anneal was increased to ~ 45 full power years compared to 2 months for the flat shield design. This implies that using the recommended shield configuration, the need for annealing during the reactor lifetime can be eliminated completely. At the same time, the peak radiation dose in the insulator is reduced allowing it also to last for the whole reactor lifetime. The peak power density in the magnet is also reduced significantly. The shield design used in this work can improve the penetration shield effectiveness significantly at no extra cost when used in ICF reactors.

The proposed shield design was used to determine the shield configuration for the improved final focussing system of HIBALL. It was found that the superconducting coils will be well protected. The radiation effects in the normal coils are several orders of magnitude lower than the design limits implying that a reduced shield thickness can be used. As a result of using two deflection sectors in the improved system, the periodic transport system is completely concealed from the direct line-of-sight of source neutrons. Consequently, neutron streaming into the periodic transport is more than four orders of magnitude less than in the previous straight beam line penetration.

#### ACKNOWLEDGEMENT

Support for this work was provided by the Kernforschungszentrum Karlsruhe and the Bundesministerium für Forschung und Technologie, Federal Republic of Germany, under research agreement with Fusion Power Associates, Gaithersburg, MD, USA.

#### REFERENCES

1. B. Badger et al., "HIBALL - A Conceptual Heavy Ion Beam Driven Fusion Reactor Study," UWFDM-450, Fusion Engineering Program, University of Wisconsin (1981).
2. S.G. Varnado and G.A. Carlson, "Considerations in the Design of Electron-Beam-Induced Fusion Reactor Systems," Nucl. Technol., 29, 415 (1976).
3. W.R. Meier and J.A. Maniscalco, "Reactor Concepts for Laser Fusion," UCRL-79694, Lawrence Livermore National Laboratory (1977).
4. "ANISN-ORNL," RSIC Code Package CCC-254, Radiation Shielding Information Center, Oak Ridge National Laboratory (1979).
5. "MORSE-CG," RSIC Code Package CCC-203, Radiation Shielding Information Center, Oak Ridge National Laboratory (1977).
6. "VITAMIN-C, 171 Neutron, 36 Gamma-Ray Group Cross Sections Library in AMPX Interface Format for Fusion Neutronics Studies," DLC-41, RSIC Data Library, Oak Ridge National Laboratory (1979).
7. "MACKLIB-IV, 171 Neutron, 36 Gamma-Ray Group Kerma Factor Library," DLC-60, RSIC Data Library, Oak Ridge National Laboratory (1979).